第 43 卷第 4 期
2024 年 8 月

红外与毫米波学报
J. Infrared Millim. Waves

Vol. 43，No. 4
August，2024

文章编号：1001-9014（2024）04-0520-06

DOI：10. 11972/j. issn. 1001-9014. 2024. 04. 011

An improved ASM-HEMT model for kink effect on GaN devices

WANG Shuai[1,2]，CHENG Ai-Qiang[2]，GE Chen[2]，CHEN Dun-Jun[1*]，LIU Jun[3]，DING Da-Zhi[4]

（1. Department of Electronic Science and Engineering，Nanjing University，Nanjing 210033，China；
2. Nanjing Electronic Devices Institute，Nanjing 210016，China；
3. Department of Electronic Information，Hangzhou Dianzi University，Hangzhou 310018，China；
4. Department of microelectronics，Nanjing University of Science and Technology，Nanjing 210094，China）

Abstract：With the analysis of experiment and theory on GaN HEMT devices under DC sweep，an improved model for kink effect based on advanced SPICE model for high electron mobility transistors（ASM-HEMT）is proposed，considering the relationship between the drain/gate-source voltage and kink effect. The improved model can not only accurately describe the trend of the drain-source current with the current collapse and kink effect，but also precisely fit different values of drain-source voltages at which the kink effect occurs under different gate-source voltages. Furthermore，it well characterizes the DC characteristics of GaN devices in the full operating range，with the fitting error less than 3%. To further verify the accuracy and convergence of the improved model，a load-pull system is built in ADS. The simulated result shows that although both the original ASM-HEMT and the improved model predict the output power for the maximum power matching of GaN devices well，the improved model predicts the power-added efficiency for the maximum efficiency matching more accurately，with 4% improved.

Key words：ASM-HEMT，DC，current collapse，kink effect

GaN器件kink效应建模研究

王 帅[1,2]，成爱强[2]，葛 晨[2]，陈敦军[1*]，刘 军[3]，丁大志[4]

（1. 南京大学 电子科学与工程学院，江苏 南京 210033；
2. 南京电子器件研究所，江苏 南京 210016；
3. 杭州电子科技大学 电子信息学院，浙江 杭州 310018；
4. 南京理工大学 微电子学院，江苏 南京 210094）

摘要：本文通过分析耗尽型GaN器件kink效应，基于ASM-HEMT提出了一种改进模型。该模型考虑到漏源电压、栅源电压与kink效应的关系，不仅能够准确模拟电流崩塌和kink效应发生时的漏源电流趋势，而且精准拟合了不同栅源电压下kink效应发生时对应的漏源电压值$V_{ds\text{-}k}$，表明改进模型能够准确表征GaN器件在整个工作电压范围内的直流特性，拟合误差在3%以内。为了验证改进模型的精确度，利用ADS负载牵引仿真电路进行了模型仿真，仿真结果显示，改进模型最佳效率匹配时的功率附加效率精确度比原始ASM-HEMT模型提高了4%。

关 键 词：ASM-HEMT；直流特性；电流崩塌；kink效应

中图分类号：TN385　　**文献标识码**：A

Introduction

Gallium Nitride high electron mobility transistors（HEMTs）have promising prospects for high frequency，high voltage and high power applications，due to their unique advantages of the material[1-2]. As the bridge between technological process and circuit design，models

---

Received date：2023-09-03，**revised date**：2023-11-03　　**收稿日期**：2023-09-03，**修回日期**：2023-11-03

Foundation items：Supported by the National Key R&D Program of China（2022YFF0707800，2022YFF0707801），and Primary Research & Development Plan of Jiangsu Province（BE2022070，BE2022070-2）

Biography：WANG Shuai（1982-），male，Nanjing，professor. Research area involves microwave power devices. E-mail：wangshuai625@126. com

[*] **Corresponding author**：E-mail：djchen@nju. edu. cn

for GaN devices are critical. So far, behavioral models, empirical models and physical models have been reported[3-5]. Among these, ASM-HEMT (Advanced SPICE Model for HEMT), a physical surface-potential-based model, can accurately characterize the electrical characteristics of GaN devices with technological structure and physical mechanism well combined. Currently, ASM-HEMT has developed into the mainstream and been certified as the industry standardization[6].

As an intrinsic reliability problem of GaN devices, kink effect features an abrupt rise in drain-source current I_{ds} after collapse at a certain drain-source voltage V_{ds}. The phenomenon deteriorates the stability of the device with a drop in the transconductance g_{m1}, an increase in the output conductance g_{ds1} as well as a shift in the threshold voltage V_{off}[7-9]. Because the kink effect on GaN devices cannot be completely eliminated, its influence in circuit design cannot be ignored. However, the current collapse and kink effect are not taken into consideration in the original ASM-HEMT. In order to more accurately characterize the performance of GaN devices, it is necessary to introduce the description of current collapse and kink effect to the model.

In this paper, an improved ASM-HEMT model for kink effect is proposed. This proposed model accurately describes the current collapse and kink effect, so as to precisely characterize the DC characteristics of GaN devices in the full operating range.

1 Theory of the improved model

1.1 The drain-source current I_{ds} model in ASM-HEMT

By solving Schrodinger's and Poisson's equations, the potential of Fermi level corresponding to two-dimensional electron gas (2DEG) at GaN/AlGaN hetero-junction can be calculated as[10]:

$$V_f = V_{go} - \frac{2V_{th}\ln\left(1 + \exp\left(\frac{V_{go}}{2V_{th}}\right)\right)}{\frac{1}{H\left(V_{goeff}\right)} + \frac{C_g}{qD}\exp\left(-\frac{V_{go}}{2V_{th}}\right)} \quad , \quad (1)$$

$$V_{go} = V_{gs} - \left(V_{off} - eta0 \cdot \frac{vdscale \cdot V_{dsx}}{\sqrt{V_{dsx}^{\ 2} + vdscale^2}}\right), \quad (2)$$

where $H(V_{goeff})$ is the function of V_{go}, C_g is the gate capacitance per unit area, q is the electronic charge, D is the density of states, V_{th} is the thermal voltage, $eta0$ and $vdscale$ are the Drain Induced Barrier Lowing (DIBL) parameters, V_{off} is the threshold voltage, and V_{dsx} = sqrt ($V_{ds}^{\ 2}$+0.01).

So the potential at the source end φ_s and the potential at the drain end φ_d are obtained as follows[11]:

$$\varphi_s = V_f + V_s \quad , \quad (3)$$

$$\varphi_d = V_f + V_{deff} \quad , \quad (4)$$

where V_s is the source voltage, and V_{deff} is the effective drain voltage.

Combining the drift-diffusion mechanism with real device effects, the drain-source current I_{ds} is given as[12]:

$$I_{ds} = I_{ds}{}' \cdot \left(V_{go} - \varphi_m + V_{tv}\right) \cdot \varphi_{ds} \quad , \quad (5)$$

$$I_{ds}{}' = \frac{W}{L} n_f C_g \mu_{eff} \frac{\left[1 + \lambda\left(V_{dsx} - V_{deff}\right)\right]}{\sqrt{1 + \theta_{sat}^{\ 2}\varphi_{ds}^{\ 2}}} \quad , \quad (6)$$

where W is the gate width, L is the gate length, n_f is the number of fingers, μ_{eff} is the effective mobility, θ_{sat} is the velocity saturation parameter, V_{tv} is the correction of V_{th}, φ_m = (φ_s+φ_d)/2, φ_{ds} = φ_d-φ_s, and λ is the channel length modulation coefficient.

1.2 The improved model for kink effect

The current collapse and kink effect can be obviously observed in the output characteristic curve of GaN devices, as shown in Fig. 1. At low V_{ds} (V_{ds}≈0-8 V), electrons are trapped, leading to a decrease in channel carriers and a drop in the drain-source current, which is current collapse. As V_{ds} continues to increase, the trapped electrons are released, resulting in a rapid increase in the drain-source current, which features as the kink effect. The drain-source voltage where the kink effect occurs, defined as $V_{ds\text{-}k}$, is marked by the red triangle in Fig. 1. Meanwhile, when V_{gs} gradually increases, $V_{ds\text{-}k}$ first drops and then increases. The above phenomenon demonstrates that both V_{ds} and V_{gs} play an important role in the current collapse and kink effect.

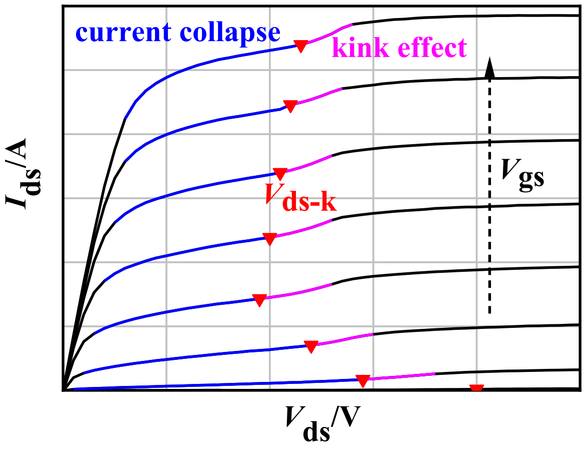

Fig. 1　Current collapse and kink effect in the output characteristics

图1　GaN HEMT器件输出特性中的电流崩塌和kink效应

On account of the shift in the threshold voltage caused by the current collapse and kink effect, V_{off} in Eq. 2 needs to be corrected. By introducing the function $CK(V_{ds}, V_{gs})$ related to V_{ds} and V_{gs}, the correction of the threshold voltage can be expressed as:

$$V_{off}{}' = \left[1 + CK\left(V_{ds}, V_{gs}\right)\right] \cdot V_{off} \quad . \quad (7)$$

The tendency of I_{ds} rapidly increasing after collapse can be modeled by a hyperbolic tangent function tanh[13], which is exactly the form of $CK(V_{ds}, V_{gs})$:

$$CK\left(V_{ds}, V_{gs}\right) = d0 \cdot \tanh\left[d1 \cdot \left(V_{ds} - V_{ds-k}\right)\right], \quad (8)$$

where $d0$ and $d1$ are fitting parameters, which determine the amplitude of current collapse and kink effect.

Considering the nonlinear relationship between $V_{ds\text{-}k}$ and V_{gs}, $V_{ds\text{-}k}$ is given as a polynomial related to V_{gs}:

$$V_{ds-k} = g0 + g1 \cdot V_{gs} + g2 \cdot V_{gs}^{2} + g3 \cdot V_{gs}^{3} + \cdots\cdots \quad , \qquad (9)$$

where gk ($k = 0, 1, 2...$) is the fitting parameter.

Substituting Eq. 7 for V_{off} in Eq. 2, the final drain-source current I_{ds} can be rewritten as:

$$I_{ds} = I_{ds}' \cdot \left[V_{gs} - \left(V_{off}' - eta0 \cdot \frac{vdscale \cdot V_{dsx}}{\sqrt{V_{dsx}^{2} + vdscale^{2}}} \right) - \varphi_{m} + V_{tv} \right] \cdot \varphi_{ds} \quad . \qquad (10)$$

2 Modeling process

2.1 Devices and the test system

Two depletion-mode GaN HEMTs used in the paper are developed by Nanjing Electronic Devices Institute with gate widths of 6×200 μm and 2×200 μm, as shown in Fig. 2.

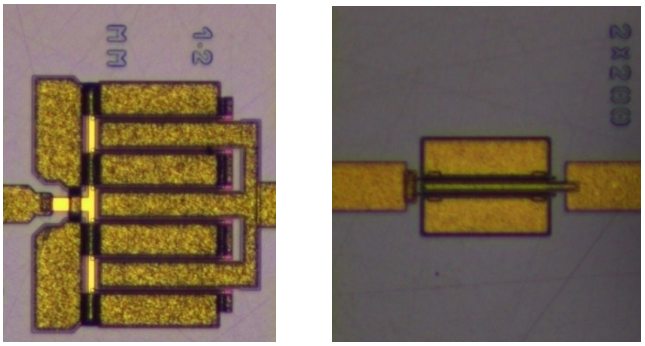
(a) (b)

Fig. 2 Photographs of D-mode GaN HEMTs: (a) the 1.2-mm-wide device;(b) the 0.4-mm-wide device
图2 耗尽型GaN HEMT器件实物图:(a) 1.2 mm GaN器件;(b) 0.4 mm GaN器件

Firstly, as shown in Fig. 3, on-wafer measurement is carried out at room temperature ($T = 300$ K) for the DC characteristics, and the measured data is obtained through the IVCAD software of Maury Company. Secondly, the improved model is realized by Verilog-A and simulated on the ICCAP software. Finally, based on the measurements, parameters of the improved model are extracted and the DC characteristics are fitted, including the output characteristics I_{ds}-V_{ds}, the output conductance (the first derivative of I_{ds} with respect to V_{ds}) g_{ds1}-V_{ds}, the transfer characteristics I_{ds}-V_{gs} and the transconductance (the first derivative of I_{ds} with respect to V_{gs}) g_{m1}-V_{gs}, measured and simulated with the value of V_{ds} varying from 0 V to 36 V in the step of 0.2 V and the value of V_{gs} changing from -4 V to 0 V in the step of 0.1 V.

2.2 Parameters extraction

For the output characteristics and the S-parameter, the fitting results of the original ASM-HEMT and the improved model are shown in Figs. 4-6.

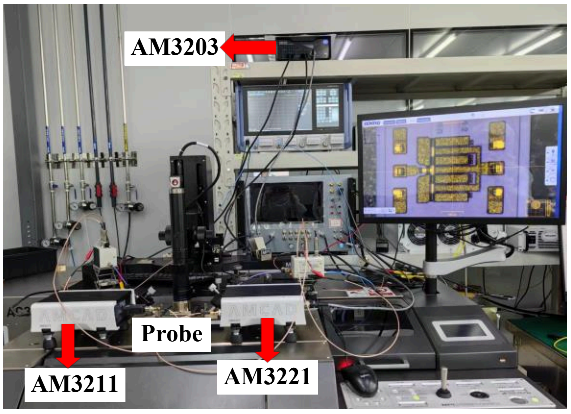

Fig. 3 The test system
图3 测试平台

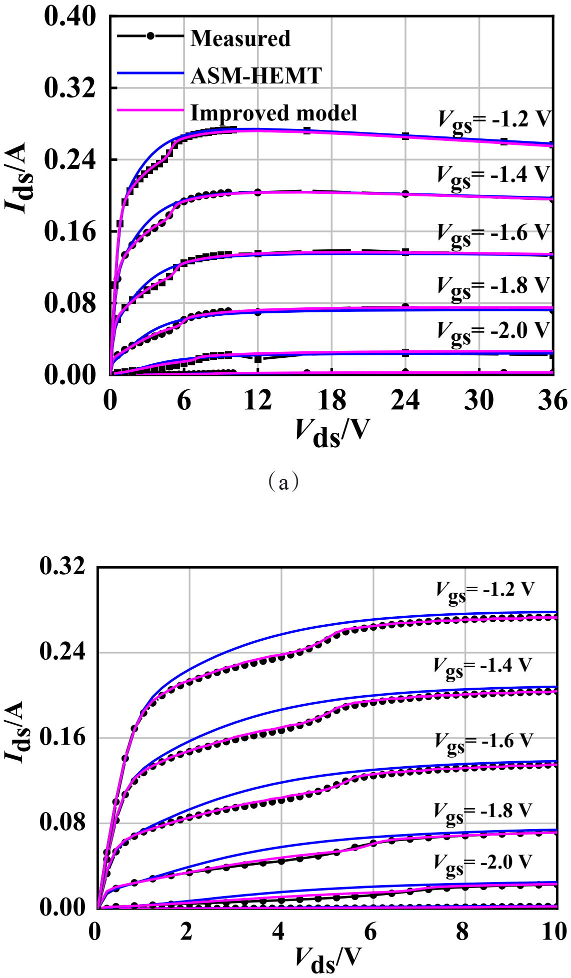

(a)

(b)

Fig. 4 The fitting result of the output characteristics I_{ds}-V_{ds} for the 1.2-mm-wide device: (a) V_{ds} ranges from 0 V to 36 V;(b) V_{ds} ranges from 0 V to 10 V
图4 1.2 mm GaN器件输出特性I_{ds}-V_{ds}拟合结果: (a) V_{ds}=0~36 V; (b) V_{ds}=0~10 V

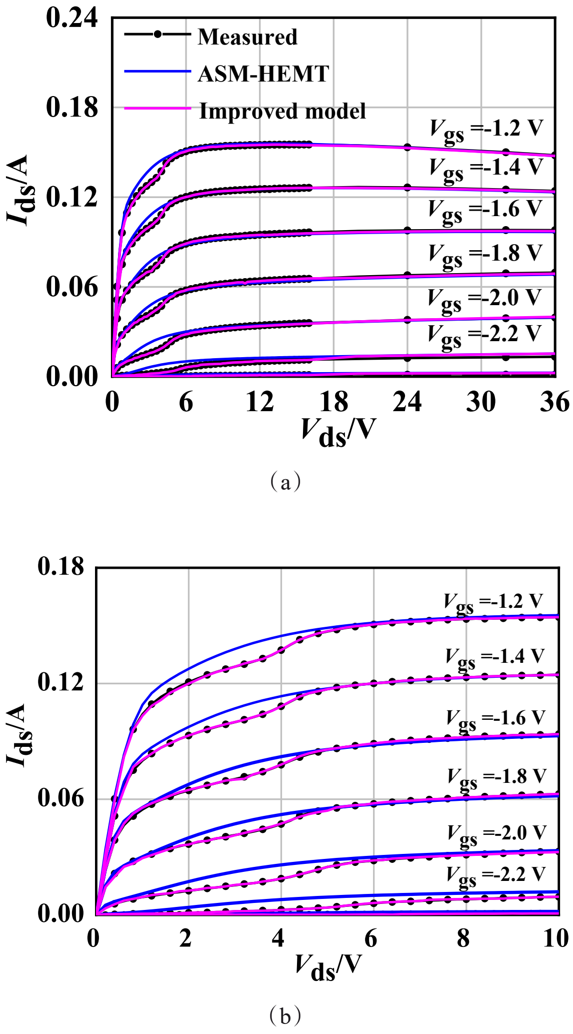

(a)

(b)

Fig. 5　The fitting result of the output characteristics I_{ds}-V_{ds} for the 0.4-mm-wide device: (a) V_{ds} ranges from 0 V to 36 V; (b) V_{ds} ranges from 0 V to 10 V

图 5　0.4 mm GaN 器件输出特性 I_{ds}-V_{ds} 拟合结果: (a) V_{ds}=0~36 V; (b) V_{ds}=0~10 V

2.2.1　Fitting of the output characteristics curves

Seen from Fig. 4(a) and Fig. 5(a), both the original ASM-HEMT and the improved model fits to the measured curve well in the saturation region, but there are obvious differences in the regions where the current collapse and kink effect occur. The accuracy of the original ASM-HEMT is insufficient, as shown in Fig. 4(b) and Fig. 5(b). For the improved model, I_{ds} behaves an abrupt rise after collapse as V_{ds} increases, and $V_{ds\text{-}k}$ under different V_{gs} is also perfect fitted.

2.2.2　Fitting of the *S*-parameter

The *S*-parameter simulation results from 400 MHz to 40 GHz of the original model and the improved model are compared with the measurements for two devices, as shown in Fig. 6.

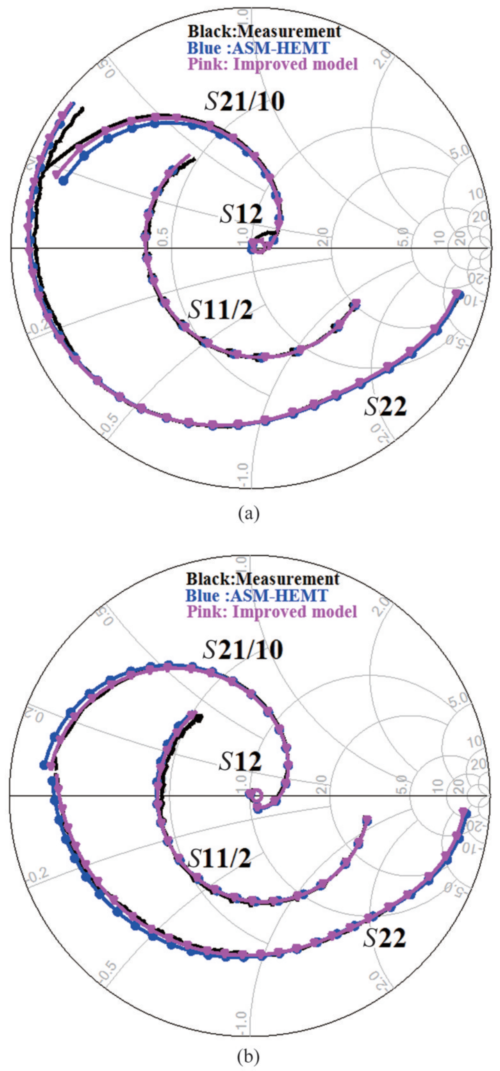

(a)

(b)

Fig. 6　The fitting result of the *S*-parameter: (a) the 1.2-mm-wide device; (b) the 0.4-mm-wide device

图 6　*S* 参数拟合结果: (a) 1.2 mm GaN 器件; (b) 0.4 mm GaN 器件

For the small signal characteristic at V_{gs} = -2.2 V and V_{ds} = 28 V, the good agreement between the measured results and both of the simulated results is obtained. Because the input is the small signal, the impact of kink effect on the RF characteristics can be ignored.

2.2.3　Final parameters

Finally, the extracted parameters are obtained in Table 1 and Table 2.

The above results indicate that the improved model can accurately describe the current collapse and kink ef-

Table 1　The extracted parameters related to the current collapse and kink effect for the 1.2-mm-wide device

表 1　1.2 mm GaN 器件电流崩塌和 kink 效应相关参数值

The fitting parameter	*d*0	*d*1	*g*0	*g*1	*g*2	*g*3	*g*4
Value	5.234 m	10	2.506	18.15 m	69.02 m	218.3 m	151.4 m

Table 2 The extracted parameters related to the current collapse and kink effect for the 0.4-mm-wide device
表2 0.4 mm GaN器件电流崩塌和kink效应相关参数值

The fitting parameter	*d*0	*d*1	*g*0	*g*1	*g*2	*g*3	*g*4
Value	21. 83 m	3. 793	3. 282	477. 5 m	584. 2 m	0. 001 m	3. 451 m

fect, and characterize the output characteristics of GaN devices with different sizes.

3 Results

The fitting result of the output conductance (V_{gs} = -1. 2 V for the 1. 2-mm-wide device in this paper) is shown in Fig. 7. It can be seen that the improved model appears a peak near V_{ds} = 4 V, which agrees with the description in Ref. [14] and is well matched with the measured data, further proving that the improved model accurately describes the current collapse and kink effect of GaN devices.

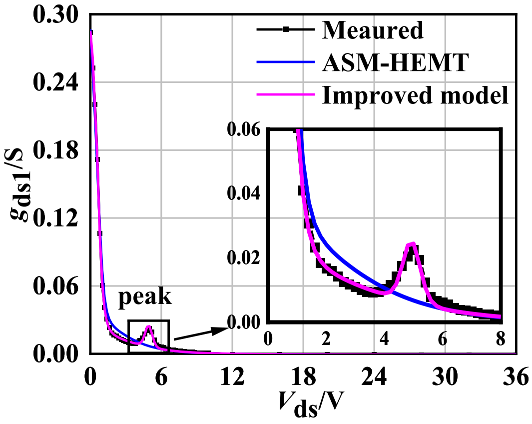

Fig. 7 The fitting result of the output conductance g_{ds1}-V_{ds}
图7 输出电导g_{ds1}-V_{ds}拟合结果

Figure 8 shows the fitting results of the transfer characteristics at V_{ds} = 4 V and V_{ds} = 28 V. The original ASM-HEMT fits well where V_{ds} is high (V_{ds} = 28 V for the 1. 2-mm-wide device in this paper), but the fitting error is large where V_{ds} is low (V_{ds} = 4 V for the 1. 2-mm-wide device in this paper), while the improved model can achieve an excellent fit under all V_{ds}. Accordingly, the transconductance of the improved model agrees well with the measured data, as shown in Fig. 9, indicating that the improved model accurately characterizes the transfer characteristics of GaN devices by introducing parameters related to the current collapse and kink effect.

According to the above results, the improved model perfectly fits the kink effect of GaN devices. Clearly, the improved model accurately describes the current collapse and kink effect, so as to precisely characterize the DC characteristics of GaN devices in the full operating range.

To further verify the accuracy of the improved model, a load-pull simulation is built in ADS, as shown in Fig. 10. The improved model is validated by simulating the large signal behavior at 3 GHz and I_{dsq}= 12 mA at V_{ds} = 28 V, with the input power Pin swept from 1 dBm to 24 dBm.

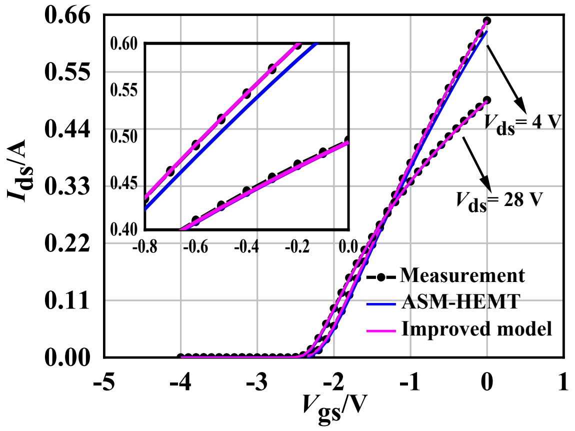

Fig. 8 The fitting result of the transfer characteristics I_{ds}-V_{gs}
图8 转移特性I_{ds}-V_{gs}拟合结果

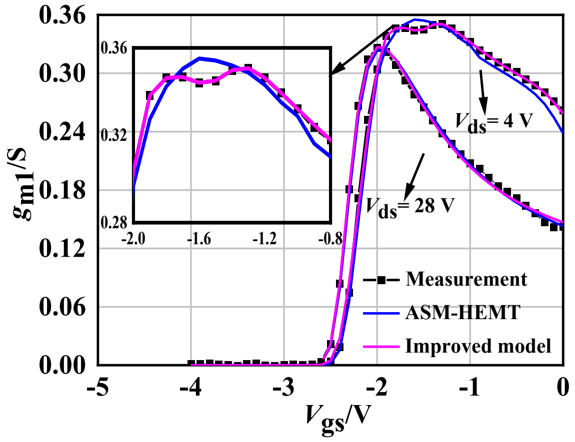

Fig. 9 The fitting result of the transconductance g_{m1}-V_{gs}
图9 跨导g_{m1}-V_{gs}拟合结果

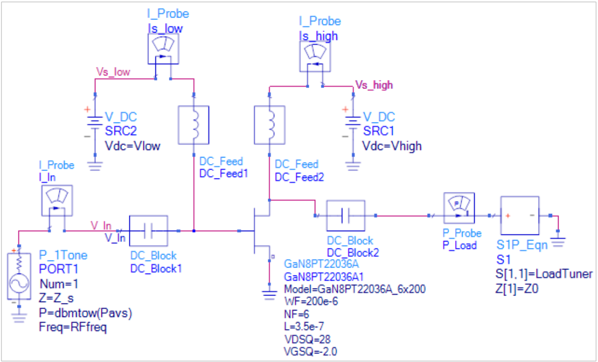

Fig. 10 Schematic diagram of the load-pull simulation in ADS
图10 ADS负载牵引仿真原理图

As shown in Fig. 11, both the original ASM-HEMT and the improved model can predict the output power for the maximum power matching of GaN devices well. How-

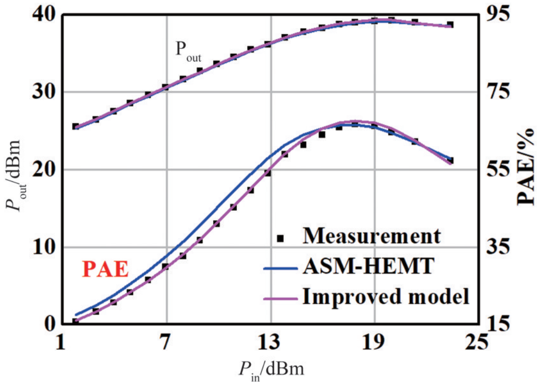

Fig. 11 Simulated and measured P_{out} for the maximum power matching and PAE for the maximum efficiency matching

图 11 最佳功率匹配时输出功率 P_{out}、最佳效率匹配时功率附加效率 PAE 的仿真结果和测试结果

ever, compared with the original ASM-HEMT, the improved model predicts the power-added efficiency (PAE) for the maximum efficiency matching more accurately, with 4% improved, which has a good agreement with the measured result.

4 Conclusions

An improved model for kink effect based on ASM-HEMT is presented in this paper, considering the impact of V_{ds} and V_{gs}. Validated with the experimental data, the improved model can accurately describe the current collapse and kink effect, and more accurately characterize the DC characteristics of GaN devices in the full range of voltage, with the fitting error less than 3%. Compared with the original ASM-HEMT, the improved model predicts the power-added efficiency for the maximum efficiency matching more accurately without changing the accuracy of the output power for the maximum power matching. The improved model is of great guiding significance for the accurate design of high-performance GaN amplifiers, and can also play a crucial role in reducing circuit design costs and shortening the product development cycle. Since GaN devices used in the paper adopt a process of 0.35 μm, they are not suitable for millimeter waves. To further broaden the applicability of the improved model, GaN devices for higher frequency will be studied in the future.

References

[1] Mishra U K, Shen L, Kazior T E, *et al*. GaN-based RF power devices and amplifiers [J]. *Proceedings of the IEEE*, 2008, **96** (2): 287-305.

[2] Ma S, Liu J, Wang J, *et al*. Comparison of two standard physical models of GaN HEMTs: MVSG and ASM [C]. 2021 IEEE MTT-S International Wireless Symposium (IWS), Nanjing, China, 2021: 1-3.

[3] Ghosh S, Sharma K, Agnihotri S, *et al*. Modeling of temperature effects in a surface-potential based ASM-HEMT model [C]. 2014 IEEE 2nd International Conference on Emerging Electronics (ICEE), Bengaluru, India, 2014: 1-4.

[4] Khandelwal S, Chauhan Y S, Fjeldly T A, *et al*. ASM GaN: Industry standard model for GaN RF and power devices—Part 1: DC, CV, and RF model [J]. *IEEE Transactions on Electron Devices*, 2019, **66**(1): 80-86.

[5] Miller N C, Moser N A, Fitch R C, *et al*. Accurate nonlinear GaN HEMT simulations from X- to Ka-Band using a single ASM-HEMT model [C]. 2021 IEEE 21st Annual Wireless and Microwave Technology Conference (WAMICON), FL, USA, 2021: 1-4.

[6] Kellogg K, Khandelwal S, Craig N, *et al*. Improved charge modeling of field-plate enhanced AlGaN/GaN HEMT devices using a physics based compact model [C]. 2018 IEEE BiCMOS and Compound Semiconductor Integrated Circuits and Technology Symposium (BCICTS), CA, USA, 2018: 102-105.

[7] Meneghesso G, Zanon F, Uren M J, *et al*. Anomalous kink effect in GaN high electron mobility transistors [J]. *IEEE Electron Device Letters*, 2009, **30**(2): 100-102.

[8] CAO Meng-Yi, LU Yang, WEI Jia-Xing, *et al*. An improved EEHEMT model for kink effect on AlGaN/GaN HEMT [J]. *Chinese Physics B*, 2014, **23**(8): 452-456.

[9] FU Li-Hua, LU Hai, CHEN Dun-Jun, at al. Field-dependent carrier trapping induced kink effect in AlGaN/GaN high electron mobility transistors [J]. *Applied Physics Letters*, 2011, **98**(17): 173508-1-3.

[10] Khandelwal S, Chauhan Y S, Fjeldly T A. Analytical modeling of surface-potential and intrinsic charges in AlGaN/GaN HEMT devices [J]. *IEEE Transactions on Electron Devices*, 2012, **59**(10): 2856-2860.

[11] Ghosh S, Ahsan S A, Dasgupta A, *et al*. GaN HEMT modeling for power and RF applications using ASM-HEMT [C]. 2016 3rd International Conference on Emerging Electronics (ICEE), Mumbai, India, 2016: 1-4.

[12] Dasgupta A, Ghosh S, Chauhan Y S, *et al*. ASM-HEMT: Compact model for GaN HEMTs [C]. 2015 IEEE International Conference on Electron Devices and Solid-state Circuits (EDSSC), Singapore, 2015: 495-498.

[13] Curtice W R, Ettenberg M. A nonlinear GaAs FET model for use in the design of output circuits for power amplifiers [J]. *IEEE Transactions on Microwave Theory and Techniques*, 1985, **33** (12): 1383-1394.

[14] Khade RP, Sarkar S, DasGupta A, *et al*. Origin of the kink effect in AlInN/GaN high electron-mobility transistor [J]. *Journal of Applied Physics*, 2021, **130**(20): 205707.